

# Numerical Analysis of Laminar Flames of Methanol Soaked Wick under the Configuration of Heterogenous Cross Flow

Hariharan Da, Duraivelu Kb,\*

<sup>a</sup> Department of Mechanical, Aerospace and Civil Engineering, University of Manchester, Manchester, United Kingdom.

<sup>b</sup> Department of Mechanical Engineering, SRM Institute of Science and Technology, Kattankulathur, India.

## Keywords:

Methanol  
Short Kinetics Mechanism  
Flame Structure  
Cross Flow  
Mass Burning Rate

\* Corresponding author:

Duraivelu K   
E-mail:  
[duraivek1@srmist.edu.in](mailto:duraivek1@srmist.edu.in)

Received: 11.10.2024.

Revised: 16.12.2024.

Accepted: 20.12.2024.

## ABSTRACT

Methanol economy is considered to be a potential future economy which offers an alternative to the depleting fossil fuels and proposed hydrogen economy for the transportation fuel. Motivated from this interest, a research conducted on estimation of characteristics of laminar methanol flames using numerical simulation model is discussed in this article. The study involves multi-component diffusion, variable physical and thermal entities. Interface conditions at the fuel pool surface are introduced with a user-defined function under heterogeneous flames in a cross flow. The results simulated using Ansys are compared with the experimental results reported in the literature. This article presents in detail the flame characteristics in respect of mass burning rate, flow rate, maximum temperature and its location, and species fields.

© 2025 Journal of Management and Engineering Sciences



## 1. INTRODUCTION

It is very important to estimate and fix the rate at which burning of fuel takes place in order to ensure the stay of reactants inside the combustion chamber for a sufficient period so the combustion reaction would be completed and efficiency of combustion could be achieved. Similarly, it is essential to understand the nature

of a flame which is termed as an exothermic reaction taking place at the interface of an oxidizer and a gaseous fuel over a shorter distance. To ensure the laminar flame with a smooth flame front, the gas flow is required to be kept laminar. The rate at which reactants mix determines the flame speed. In a calm combustible mixture, the flame is ignited that spreads outward from the ignition source at the

speed of laminar flame. The flame will transit into a detonation state within sufficient volume and create a pressure rise. Velocity of gaseous fuel and its temperature contours in the neighbourhood of the diffusion flame over fuel surface play a role in heat and mass transfer rate and chemical reaction phenomena. Data on these phenomena is much required to envisage the flame stability, rate of fuel consumption, etc. The relationship between the gas velocity and various temperature profiles are thoroughly studied in this research, to get a clear picture of burning of methanol fuel in a laminar state.

Flame speed and fuel mixture decides the flame temperature. Fuel mixture curve indicates the rich and lean limits of flammability. The flame temperature is found to be higher closer to stoichiometric mixture and lower flammability limits. The differential form of the conservative equations is required to be used to ascertain the flame speed [1]. The rate of chemical reaction and heat transfer of the fuel mixture determine the propagation rate of the laminar flame through a combustible mixture. When the liquid fuel and air stream are physically separate, the diffusion flames happen. The process of mixing the fuel with oxidizer limits the energy release rate of the mixture. The behaviour of the diffusion flames is influenced by the chemical kinetics. There are no fundamental flame speed governing diffusion flames, unlike premixed laminar flames. Flowing gases, vaporization of liquid fuels, devolatilization of solid fuels are good examples for the occurrence of diffusion flames.

Since methanol finds its way into burners of different kinds including household burners besides its application in internal combustion engines, many governments are planning to enhance methanol as an alternate fuel for crude oil imports. This idea induces various studies of making methanol from coal and biomass. In this research, an attempt has been made to understand the detailed flame characteristics of methanol in a heterogeneous cross flow configuration. The study includes mass burning rate, flame speed and extent, distribution of reaction zones.

## 2. LITERATURE REVIEW

Extensive literature is available on the experimental analysis of methanol flames under

various air-flow environments. In this section, a few important literatures highlighting the profiles of velocity and temperature of laminar flames are discussed with respect to the topic of this article.

Hirano and Kinoshita [2] carried out the experiment with the air stream passing above the surface of liquid fuel pool to explain the distinction of mass burning rate of methanol with the variation of air flow velocity. Wood et al [3] observed the uniform mass flux for the stable case for the wide-ranging shapes of burners at various air flow velocities. However, the burning rate is reliant on the extent of the flame along the direction of the stream. Hu et al [4] hinted that the burning rate increases at higher air flow velocity. Traditional convection from the flame influenced the heat-mass transfer rate much at lower air flow velocity, whereas radiation effect dominated the heat transfer rate at higher air flow velocity. Ahmad and Faeth [5] carried the experiment with vertical wicks soaked with methanol. The flame length standardised with the length of the pyrolysis region was noted to be high for the laminar flames compared with turbulent flames. Weckman and Strong [6] examined the Prandtl and Reynolds numbers for the structure of a turbulent flame. The air entry into the burning zone was deduced with the support of contours of fixed velocity and radial contours of velocity at different altitudes above the methanol liquid surface.

Similarly, extensive Literature is available on the numerical analysis of methanol flames. Prasad et al [7] projected the organisation of a methanol flame numerically using global single step chemistry. They predicted the temperature profiles at different altitudes from the methanol liquid pool using the numerical model and compared the same with the experimental values. Des Jardin et al [8] provided a mathematical model for a methanol flame in a 31cm diameter methanol fuel surface with a universal single step chemistry model, to discuss the organisation of a methanol flame using different profiles of temperature and velocity. Raghavan et al [9] also verified the theory of Emmons for a cross flow diffusion flame above a methanol surface using a single step model. Ali et al [1] also reviewed the methanol flame characteristics and mass burning rate with a 2D model developed with the universal single step model. They conducted an

experiment to study the transient flame distributed over 1m length methanol fuel surface and compared their predicted results of flame rate using the developed 2D model, with their experimental data [10].

Westbrook and Dryer [11] suggested a scheme of reaction with 84 elementary reactions and 26 species to envisage the features of a laminar flame. Seshadri et al [12] suggested a model with 37 elementary reactions and 15 species for the reverse flow of methanol flames in an axisymmetric region. Eugolfopoulos et al [13] worked on a reaction mechanism with 171 elementary reactions and 30 species of methanol and compared the performance of a flame structure with experimental data. San Diego mechanism [14] was presented with 58 species and 266 fundamental reactions to study the obstruction of flames in the existence of suppressants. To forecast the flame structure and destruction strain rates, Seisser et al [15] developed another model and offered a reduced reaction mechanism for the methanol ignition. Tarazzo et al [16] predicted the performance of non-premixed and premixed methanol flames, using 38 elementary reactions and 18 species. Sharanya Nair and Raghavan [17] could predict the qualitative characteristics [18-20] of the methanol flame extinction profiles of species.

### 3. METHODOLOGY

In this study, simulations were performed using a pressure based 2D solver in Ansys FLUENT. Only the gaseous phase was explained with the suitable interface conditions stated at the surface of methanol fuel, for the simulation which involved heterogeneous flames and condensed fuel surface. This could be achieved keeping the burning steady and fuel surface planar cum non-regressing. The reaction scheme with 5 species of CH<sub>3</sub>OH, O<sub>2</sub>, H<sub>2</sub>O, CO<sub>2</sub>, N<sub>2</sub> and one elementary reaction for a viscous laminar methanol flame model was used in CHEMKIN format. A user defined function (UDF) to define the losses of radiation due to participation of species was incorporated in the model. The following Maxwell Stefan equation (1) was solved in the background of Ansys FLUENT.

Scheme of Second-order central difference discretization and upwind were followed for obtaining spatial derivatives of terms of diffusion

and convection respectively. Transient terms use first order implicit solver.

$$\sum_{\substack{j=1 \\ j \neq i}}^n \frac{X_i X_j}{D_{i,j}} (\vec{V}_j - \vec{V}_i) = \vec{\nabla} X_i \frac{\vec{\nabla} T}{T} \sum_{\substack{j=1 \\ j \neq i}}^n \frac{X_i X_j}{D_{i,j}} \left( \frac{D_{Tj}}{\rho_j} - \frac{D_{Ti}}{\rho_i} \right) \quad (1)$$

To validate the experimental studies of Hirano and Kinoshita, a computational domain for a cross flow flame is used as shown in Fig. 1 [2]. In this domain, the surface of the methanol is 8 cm long. It is provided with two adiabatic walls and no-slip walls on both side and top. Air is allowed to enter into the combustion chamber with a constant velocity and the flow leaves through the free periphery on the right.

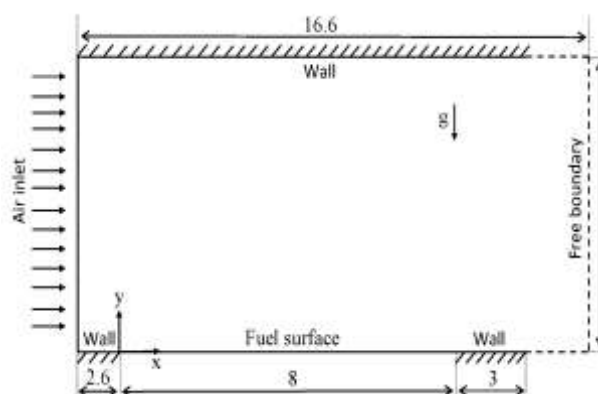


**Fig. 1.** Computational domain; all dimensions are in cm.

The boundary settings for all the stated variables are mentioned based on the nature of the boundary. At the open boundary, the flow variables are deduced from the inner cells for the stream leaving the region. For the inward flow, the velocity is computed with the pressure gradient, air-mass fractions fixed at 0.233 and 0.767 respectively. The temperature is set at 300 K. Boundary walls are configured with adiabatic and no-slip conditions. The derivatives of mass fractions of all the species are initially fixed at zero. UDF is developed to specify the boundary conditions at the liquid fuel surface, depending on the conservation of mass, momentum and energy.

The fuel surface temperature is computed based on the heat transfer from the ambient to the fuel

surface. Latent heat of vaporisation of the methanol fuel is given by (2)

$$\rho_s v_s h_{fg} = k_s \frac{\partial T}{\partial n} \quad (2)$$

The temperature gradient is calculated from the temperatures of the surface and found in the 2-interior nodes through a 3-point projection. The partial pressure is calculated using methanol specific constants of A, B, C at 8.08097, 1582.27 and 239.7 respectively mentioned in the following expression (3).

$$\text{Log}_{10} p = A - B / (C + T_s - 273.15) \quad (3)$$

The mass fraction is evaluated using the following expression (4) of Fick's law:

$$\rho_s v_s = \rho_s v_s Y_{Fs} - \rho D_{Fs} \frac{\partial Y_F}{\partial n} \quad (4)$$

The standard derivative of mass fraction at the boundary is computed through a 3-point projection. The mass fractions of all other species are computed with each of their mass flux set to zero using the procedure given in literature.

$$\rho_s v_s Y_i = \rho D_{is} \frac{\partial Y_i}{\partial n} \quad (5)$$

The computational region is split into numerous cells, evenly spread over the region. A mesh is introduced into the solver and the boundary settings are indicated. UDF for boundary settings is provided as input. The short kinetics model is specified in CHEMKIN format. The computational domain is initialised with zero velocity and 300 K temperature. The mass fraction of nitrogen and oxygen is set to 0.767 and 0.233 respectively. A cold flow imitation is performed to permit the flow of methanol and oxidiser into the combustion zone and to mix rightly, by halting the volumetric reaction terms. After 5000 iterations, the temperature of 1700K is set in the domain. Volumetric reaction terms are enabled. The case is considered to be steady when the residuals decrease to the low level of  $10^{-3}$ ,  $10^{-6}$  and  $10^{-4}$  for continuity, energy and species respectively. The simulation run is continued until the mass imbalance goes below 1%. A time gap of  $10^{-5}$  seconds is used between numbers of iterations. Each steady case is run for 100,000 iterations at the minimum. A uniform mesh of size 0.5mm and 65072 cells is configured with the

short mechanism for 5 species, to analyse the heterogeneous flames in this study.

## 4. RESULTS AND DISCUSSION

The experimental values obtained by Hirano and Kinoshita [1] are compared with the numerical results predicted in this study. The characteristics of a methanol flame in a cross-flow configuration are analysed. A grid independence study is performed by engaging even grids of 0.5x0.5 mm with a web of 65,072 cells.

### 4.1 Computation without UDF

Initially, the air velocity was set at 0.1m/s and slowly increased to 0.5m/s. The methanol vapour is allowed at the initial velocity of 0.0143m/s at 338 K. The oxygen mass fraction and the ambient temperature are considered to be at 0.233 and 300 K respectively. The UDF for the boundary conditions at the liquid methanol surface is provided in CHEMKIN format.

A cold flow simulation is performed by halting the volumetric reaction terms. The temperature of 1700 K is initialised in the region once the merging of cold flow is obtained. Volumetric reactions, thermal diffusion, multicomponent diffusion and stiff chemistry solver are switched on. The case is considered to be steady once the residuals reduce to the low value of  $10^{-2}$  for continuity and  $10^{-6}$  for energy. The temperature contour at the steady state of mass flow, at the initial air velocity of 0.1m/s is shown in Fig. 2, after running the calculation for approximately 10,000 iterations. The methanol flame is found to be unsteady at this point.

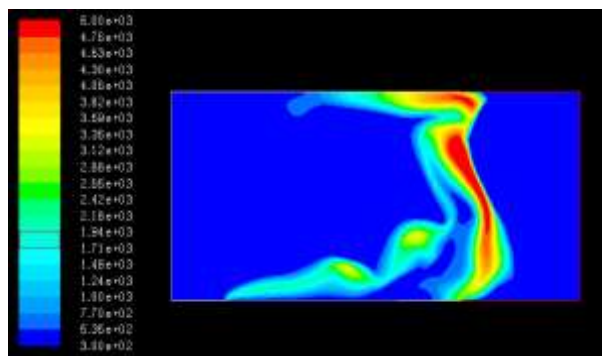


Fig. 2. Temperature contour with air velocity at 0.1m/s.

A stable state flame is obtained after increasing the air velocity to 0.25 m/s gradually and the calculation is run for 25,000 iterations. The temperature flame obtained at this stage is found to be stable at this stage. The temperature contour and the species contour are shown in Fig. 3 and Fig. 4 respectively.

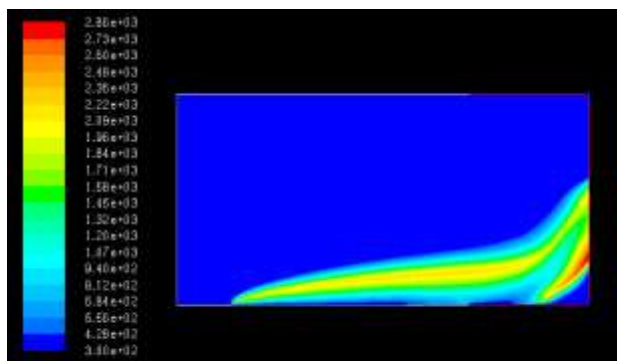


Fig. 3. Temperature contour with air velocity at 0.25m/s.

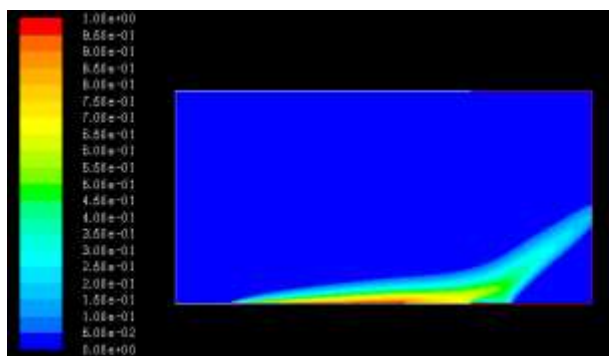


Fig. 4. Species contour with air velocity at 0.25m/s.

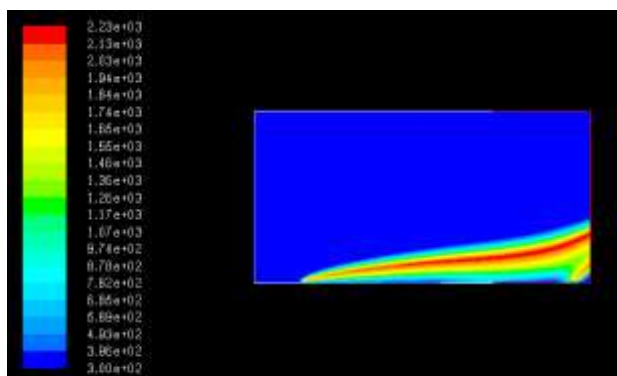


Fig. 5. Final temperature contour with air velocity at 0.5m/s.

When the simulation is run for approximately 97,000 iterations, the energy residual and continuity residual are reported to be very less at  $4.472 \times 10^{-6}$  and  $2.1011 \times 10^{-2}$  respectively. This stage is achieved when the air velocity is gradually improved to 0.5m/s. The temperature

attained at this stage is 2234.67 K. Figs. 5 and 6 represent the temperature contour and species contour at this stage.

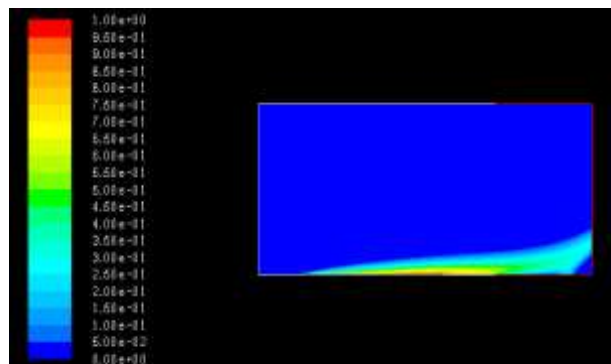


Fig. 6. Species contour with air velocity at 0.5m/s.

#### 4.2 Computation with UDF; ignoring radiation and soot models

A UDF is built to ignore soot and radiation models so as to allow the methanol liquid to evaporate under ambient conditions with specific mass fractions at certain temperatures. Alike the previous case, the air velocity is initially set at 0.1 m/s and gradually increased to 0.5 m/s. Oxygen mass fraction and ambient temperature are set at 0.233 and 300 K respectively. The steady state flame and reduced residual levels are obtained at 0.5 m/s, after running the simulation for 1,15,000 iterations. The energy residual and continuity residuals are found to be at  $1.5433 \times 10^{-5}$  and  $2.0289 \times 10^{-2}$  respectively. The temperature attained is 2106.44 K. The temperature contour and species contour attained at this stage is shown in Figs. 7 and 8 respectively.

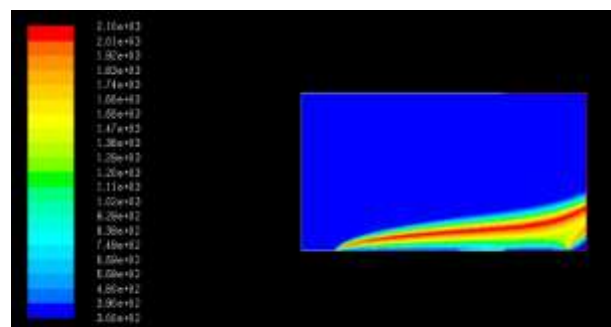


Fig. 7. Temperature contour with air velocity at 0.5m/s.

The highest value of mass fraction of 0.708 also is obtained at this stage. The range of density reported is  $1.171988 \text{ kg/m}^3 - 0.1613152 \text{ kg/m}^3$ . Also a range of pressure from 0.387487 to -0.014687 Pascal is reported at this point of time.

The density contour and pressure contour obtained are shown in Figs. 9 and 10 respectively.

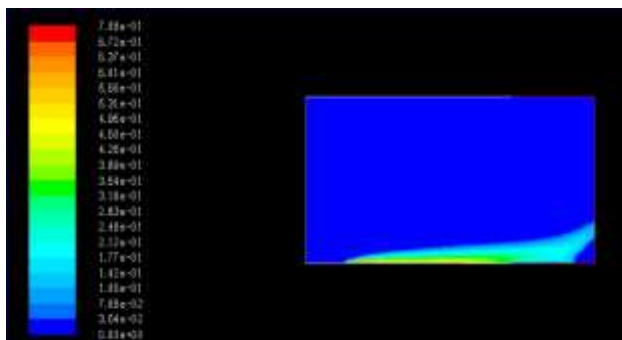


Fig. 8. Species contour with air velocity at 0.5m/s.

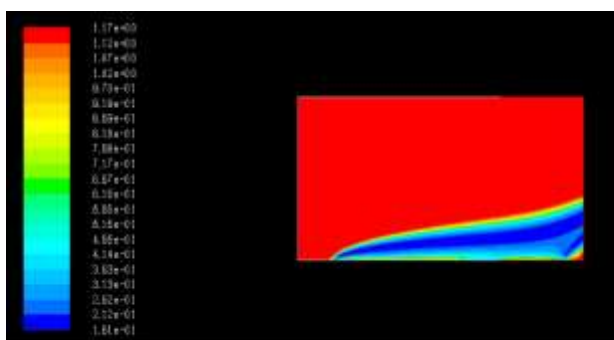


Fig. 9. Density contour with air velocity at 0.5m/s; Reference value at 1.225 kg/m<sup>3</sup>.

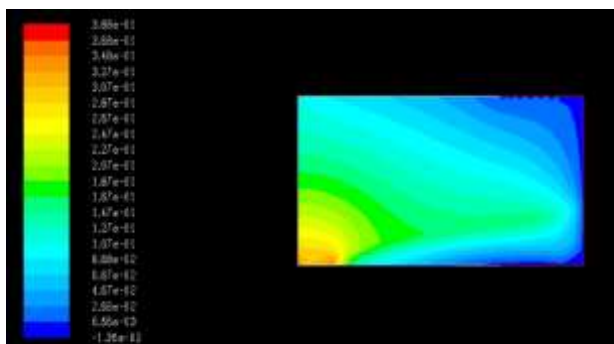


Fig. 10. Pressure contour with air velocity at 0.5m/s; Reference value at 0 pascal.

### 4.3 Computation with UDF including soot and radiation model

A UDF is built to consider the soot and radiation models. Moss Brookes and Fenimore-Jones models are selected as soot and radiation models respectively. The air velocity is initialized at 0.1m/s and increases gradually to 1.5m/s. Remarkable values for residuals and mass burning flux at the air velocity of 0.5, 0.75 and 1.5 m/s as shown in table 1, 2 and 3 respectively. The temperature contour at these three stages is shown in Figs. 11, 12 and 13 respectively.

#### Case 1: (Air velocity at 0.5m/s)

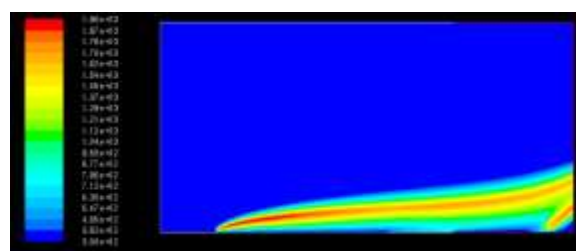


Fig. 11. Contour of Temperature (K).

Table 1. Convergence details and mass flux of case 1.

Parameter	Value
Energy Residual	1.3670 × 10 <sup>-5</sup>
Continuity Residual	1.7447 × 10 <sup>-2</sup>
Mass imbalance (%)	0.00125
Number of Iterations	102500
Mass burning flux (kg/m <sup>2</sup> s)	0.01708045

#### Case 2: (Air velocity at 0.75 m/s)

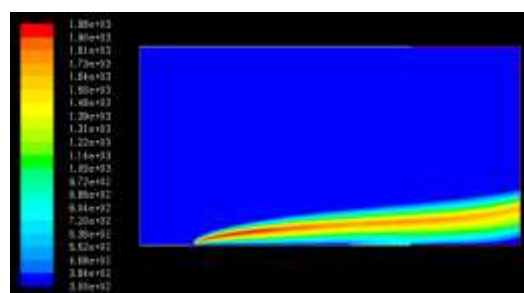


Fig. 12. Contour of Temperature (K).

Table 2. Convergence details and mass flux of case 2.

Parameter	Value
Energy Residual	1.0521 × 10 <sup>-5</sup>
Continuity Residual	2.1337 × 10 <sup>-2</sup>
Mass imbalance (%)	0.00378
Number of Iterations	170000
Mass burning flux (kg/m <sup>2</sup> s)	0.0185753625

#### Case 3: (Air velocity = 1.5 m/s)

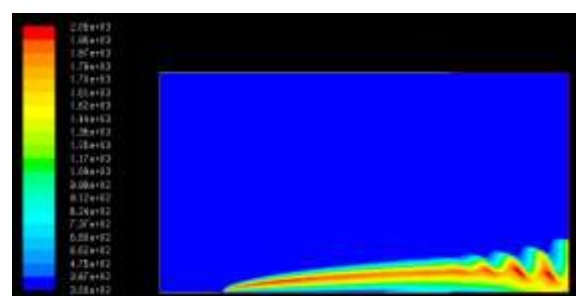
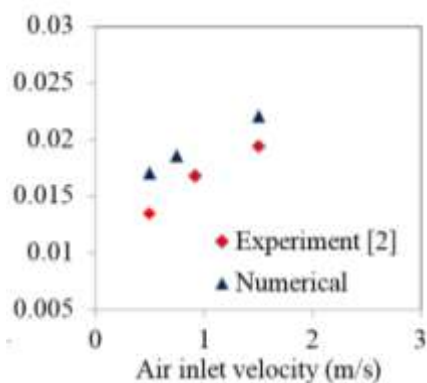


Fig. 13. Contour of Temperature (K).

**Table 3.** Convergence details and mass flux of case 3.

Parameter	Value
Energy Residual	$4.8165 \times 10^{-4}$
Continuity Residual	$8.6634 \times 10^{-2}$
Mass imbalance (%)	0.01553
Number of Iterations	194000
Mass burning flux (kg/m <sup>2</sup> s)	0.0220621125

A comparison analysis is carried out between the experimental results and the results predicted through the numerical model. Fig. 14 and 15 give the comparison of experimental values with simulated values of mass burning flux and the maximum temperature attained at specific locations in the burning region.



**Fig. 14.** Mass burning flux for different air velocities.

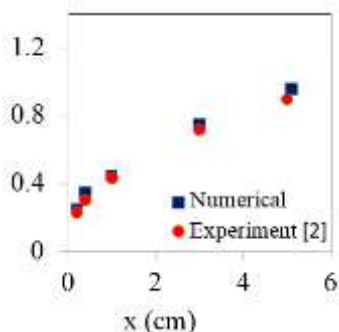
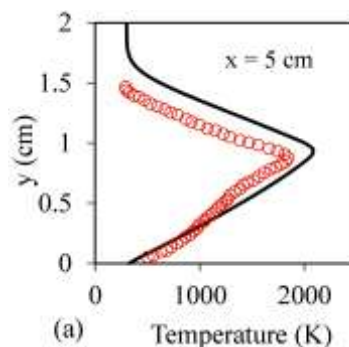
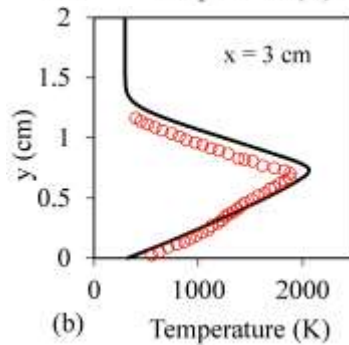


**Fig. 15.** Comparison of y-locations of maximum temperature at definite x-locations at 0.5m/s air velocity.

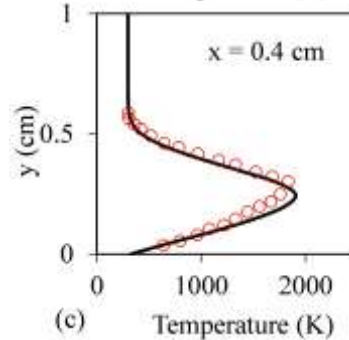
Similarly, a comparison analysis of location of maximum temperature simulated by the numerical model with that of experiments conducted is shown diagrammatically in fig. 16. It is obvious that the simulation model discussed in this study is able to capture the locations of maximum temperatures very nearer to the experimental results reported.



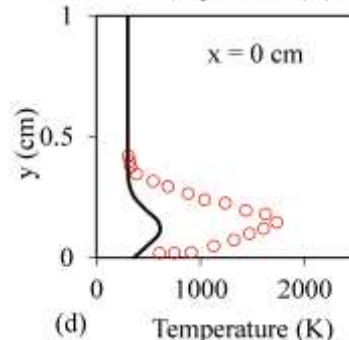
(a) Temperature (K)



(b) Temperature (K)



(c) Temperature (K)



(d) Temperature (K)

— Numerical    ○ Experiment [3]

**Fig. 16.** (a) Temperature profile along y-axis at x = 5cm (b) x = 3cm, (c) x = 0.4cm, (d) x = 0cm. Air velocity is at 0.5 m/s.

It is clear that the temperature is increasing from methanol pool surface to reaction region and decreasing to the ambient region. The numerical model presented in this study is found to be potential enough to capture the maximum temperature and its locality correctly. There are some variations found in the results obtained through the numerical model with the

experimental results in determining the temperatures at different x-locations from the prominent edge of the fuel surface. However, the temperatures projected by the simulation model are quite matching with that of the experimental results at farther x-locations from the methanol pool.

## 5. CONCLUSION

Developing countries are now taking initiatives to practice methanol as a substitute fuel in domestic and industrial domains as the usage of methanol is found to be economical comparatively. However, it needs a better understanding of methanol burning in all these application domains. Also, conducting experiments on this is quite expensive and hazardous. Numerical analysis is relatively cheaper and safe. Hence, various numerical models are required to be developed to predict the optimum values of air flow velocity and mass burning flux to obtain the steady state flame, the maximum flame temperature at the required location, the lower residual values, etc. Even some of these data are difficult to be obtained through experimental methods. However, a careful choice of model parameters is necessary for numerical models also. So, a short chemical kinetics model with 1 fundamental reaction and 5 species is proposed in this study. The simulation of cross-flow methanol diffusion flames reported in this study is found capable of capturing the profiles of temperature and flow fields, closer to the experimental results stated in the literature.

### List of symbols

X	Mole fraction
D <sub>ij</sub>	Binary mass diffusion
V	Diffusion velocity
ρ	Species density
DT	Thermal diffusion coefficient
T <sub>s</sub>	Liquid surface temperature
v	Stefan velocity
k	Thermal conductivity
h <sub>fg</sub>	Latent heat of vaporisation of the liquid fuel

## REFERENCES

[1] S.M. Ali, V. Raghavan and S. Tiwari, 2010, "A study of steady laminar diffusion flame over methanol pool surface", *International Journal*

*Heat Mass Transfer*, vol. 53, no.21, pp. 4696–4706, 2010, doi: 10.1016/j.ijheatmasstransfer.2010.06.022.

- [2] T. Hirano and M. Kinoshita, "Gas velocity and temperature profiles of a diffusion flame stabilized in the stream over liquid fuel", *Symposium (International) on Combustion*, vol. 15, pp. 379–387, 1975, doi: 10.1016/S0082-0784(75)80312-2.
- [3] J. Woods, A. Briana and L.W. Kostuik, "Effects of transverse air flow on burning rates of rectangular methanol pool fires", *Combustion and Flame*, vol. 146, pp. 379–390, 2006, doi: 10.1016/j.combustflame.2006.02.007.
- [4] L.H. Hu, S. Liu, W. Peng and R. Huo, "Experimental study on burning rates of square/rectangular gasoline and methanol pool fires under longitudinal air flow in a wind tunnel", *Journal of Hazardous Materials*, vol. 169, pp. 972–979, 2009, doi: 10.1016/j.jhazmat.2009.04.050.
- [5] T. Ahmad and G.M. Faeth, "Turbulent wall fires", *Symposium on Combustion*, vol. 17, no.1, pp. 1149–1160, 1979, doi: 10.1016/S0082-0784(79)80109-5.
- [6] E.J. Weckman and A.B. Strong, "Experimental investigation of the turbulence structure of Medium-Scale methanol pool fires", *Combustion and Flame*, vol. 105, no. 3, pp. 245–66, 1996, doi: 10.1016/0010-2180(95)00103-4.
- [7] K. Prasad, C. Li, K. Kailasnath, C. Ndubizu, R. Ananth and P.A. Tatem, "Numerical modelling of methanol liquid pool fires", *Combustion Theory and Modelling*, vol. 3, pp. 743–768, 1999, doi: 10.1016/0010-2180(95)00103-4.
- [8] P. E. DesJardin, T. M. Smith and C. J. Roy, "Numerical simulation of methanol pool fire, American Institute of Aeronautics and Astronautics", AIAA 2001-0636, USA. 2001, doi: 10.2514/6.2001-636.
- [9] V. Raghavan, A.S. Rangwala and J.L. Torero, "Laminar flame propagation on a horizontal fuel surface: verification of classical Emmons solution", *Combustion Theory and Modelling*, vol. 13, pp. 121–141, 2009, doi: 10.1080/13647830802483729.
- [10] S.M. Ali, V. Raghavan, K. Velusamy and S. Tiwari, "A numerical study of concurrent flame propagation over methanol pool surface", *Journal of Heat Transfer*, vol. 134, pp. 1–9, 2012, doi: 10.1115/1.4005111.
- [11] C.K. Westbrook and F.L. Dryer, "Comprehensive mechanism for methanol oxidation", *Combustion Science and Technology*, vol. 20, pp 125–140, 1979, doi: 10.1080/00102207908946902.

- [12] K. Seshadri, C. Trevino and M.D. Smooke, "Analysis of the structure and mechanisms of extinction of a counterflow methanol-air diffusion flame", *Combustion Science and Technology*, vol. 76, no. 2, pp. 111-32, 1989, doi: 10.1016/0010-2180(89)90061-8.
- [13] F.N. Eugolfopoulos, D.X. Du and C.K. Law, "A comprehensive study of methanol kinetics in freely-propagating and burner-stabilized flames, flow and static reactors, and shock tubes" *Combustion Science and Technology*, vol. 83, no.1, pp. 33-75, 2007, doi: 10.1080/00102209208951823.
- [14] Forman A Williams, Kalyanasundaram Seshadri and Robert Cattolica, "Chemical-Kinetic Mechanisms for Combustion Applications", *Mechanical and Aerospace Engineering (Combustion Research)*, vol. 858, pp. 534-40, 2011.
- [15] R. Seiser, K. Seshadri and F.A.Williams, "Detailed and reduced chemistry for methanol ignition", *Combustion and Flame*, vol. 158, no. 9, pp. 1667-72, 2011, doi: 10.1016/J.COMBUSTFLAME.2011.02.008.
- [16] E.F. Tarrazo, M.S. Sanz, A.L. Sanchez and F.A. Williams, "A multipurpose reduced chemical kinetic mechanism for methanol combustion", *Combustion Theory and Modelling*, vol. 20, no.4, pp. 613-631, 2016, doi: 10.1080/13647830.2016.1162330.
- [17] Sharanya Nair and V. Raghavan, "Numerical study of methanol flames in laminar forced convective environment using short chemical kinetics mechanism", *Combustion Theory and Modelling*, vol. 24, no.2, pp. 279-306, 2019, doi: /10.1080/13647830.2019.1677943.
- [18] Duraivelu K and Suryaprakasa Rao K, "House of quality in Quality Gap Analysis", *Journal of the Institution of Engineers (India), Part PR: Production Engineering Division*, vol. 87, no. 2, pp. 37-41, 2007.
- [19] Duraivelu K and Suryaprakasa Rao K, "ProducQual-A Conceptual model for quality gap analysis across PLC", *Journal of the Indian Institute of Science*, vol. 86, no. 2, pp. 113-124, 2006.
- [20] Duraivelu K, "Quality metrics for Information Systems", *Opsearch*, vol. 41, no. 3, pp. 200-207, 2004, doi: 10.1007/BF03398845.